CHAPTER 2

Experimental and computational methods

2.1 Introduction

This chapter presents the experimental and computational procedural particulars of the research carried out in this thesis. The details of the instruments used in the experimental part have also been discussed. Moreover, it gives the general methodologies for determining catalytic and photocatalytic organic pollutant degradation activities of the prepared nanomaterials. Finally, the chapter explains the computational techniques utilized in the thesis.

2.2 Experimental part

2.2.1 Materials characterization techniques with instrumentation details

2.2.1.1 Powder X-Ray Diffraction (XRD)

XRD is a rapid and non-destructive quantitative technique primarily used to identify crystalline phases, crystallite size, and strains in the material. The powder XRD patterns of synthesized catalyst in the thesis were examined using Rigaku Miniflex 600 Desktop X-Ray Diffraction System (RIGAKU Corporation, Japan) shown in figure 2.1. The instrument consists of an X-ray generation source, optics, goniometer, and detector. All XRD measurements in this thesis used Cu Kα radiation (λ= 1.54 Å). Generally, diffraction data were recorded for 2θ angles between 5° and 80° at the scan rate of 3° per minute. The peaks in the XRD patterns were matched with JCPDS files for phase identification. The interplanar d-spacing was calculated using Bragg's equation (Equation 2.1).

$$n\lambda = 2d \sin \theta \tag{2.1}$$

Where 'n' is the order of reflection, λ represents the wavelength of incident X-ray radiation, and θ (Bragg angle) is the angle between the incident and the crystallographic plane.

Figure 2.1 XRD diffractometer (Model: Mini Flex 600).

2.2.1.2 Fourier Transform Infrared Spectroscopy (FTIR)

FTIR spectroscopy, an analytical technique for functional group identification, was used to analyze organic materials and certain inorganic materials in this thesis. It provided specific information about the involvement of certain functional groups in bonding between two molecular structures [Titus et al. (2019)]. The FTIR spectra of all samples were recorded on Nicolet iS5 (THERMO ESI) (shown in figure 2.2) in the range of 4000-400 cm^{-1} with a

resolution of 0.09 cm^{-1}. Each powder sample was mixed with KBr to form the pellets subjected to FTIR spectroscopy.

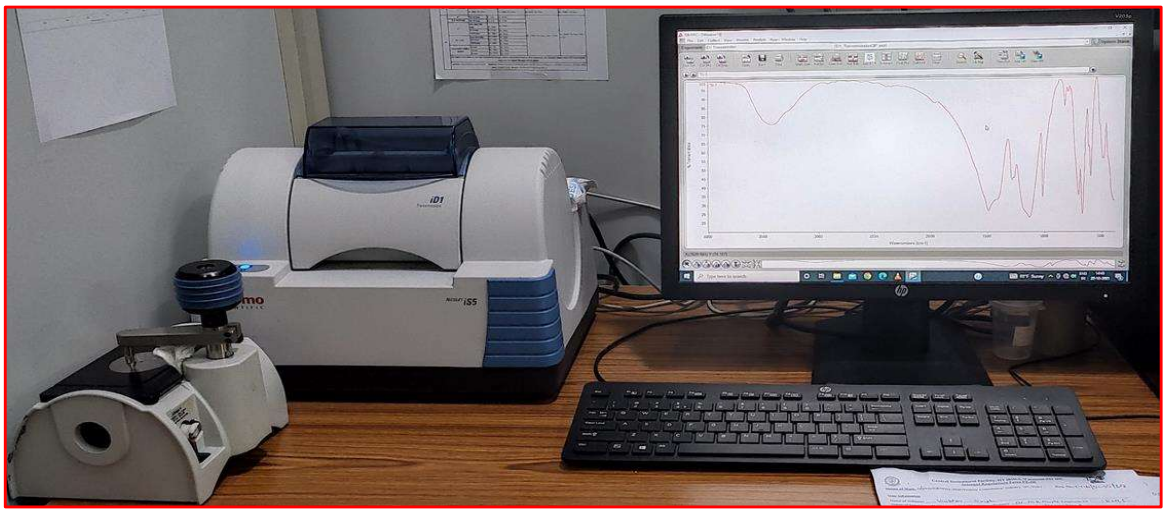

Figure 2.2 FTIR spectrophotometer (Model: Nicolet iS5).

2.2.1.3 Transmission Electron Microscopy (TEM)

TEM is a potent tool for imaging nanoscale features of material [Smith (2015)] as well as for deciphering phase-specific crystallographic details. It provides details about the morphological features such as the shape and size of particles making up a material. High-resolution TEM can be used to interpret the different phases in a nanocomposite.

In the present thesis, powder samples for TEM imaging were re-dispersed in an ethanol solution, sonicated for about half an hour, and sufficiently diluted. One drop of the sonicated sample was mounted on the carbon-coated Cu grid (400 mesh size). The grid was dried for 24 hours in a vacuum oven. The TEM grid was examined by a Tecnai G2 20 TWIN (FEI company) electron microscope (shown in Figure 2.3) equipped with a magnified CCD camera that operated voltage at 200 keV. The average particle size and size distribution were

obtained by proper statistical sampling of nanoparticle images using ImageJ software [Rice et al. (2013)].

Figure 2.3 Transmission electron microscope (Model: Tecnai G2 20 TWIN).

2.2.1.4 Scanning Electron Microscopy (SEM)

SEM is an imaging technique that scans focused electron beam over a surface to create an image. The electrons in the beam interact with the sample, producing various signals that can be used to obtain information about the surface topography and composition. The

SEM instruments have five main components, i.e., electron source, column down by which electrons travel with electromagnetic lenses, electron detector, sample chamber, and computer screen. The powder sample was dispersed on the carbon tape for SEM sample preparation. SEM images in this thesis were acquired using the Nova Nano SEM 450 model electron microscope, FEI Company (shown in Figure 2.4).

Figure 2.4 Scanning electron microscope (Model: Nova Nano SEM 450).

2.2.1.5 UV-Visible spectroscopy

UV-visible absorption spectroscopy is used to measure light absorbance across the ultraviolet and visible electromagnetic spectrum ranges. When incident light strikes, it can either be absorbed, reflected, or transmitted. The absorbance of radiation in the UV-visible spectrum causes electronic excitation, which refers to the transition of molecules from a low-

energy ground state to an excited state. These include electron excitation from non-bonding (n), or a π-orbital (π), to an antibonding π–orbital (π*) or antibonding σ-orbital (σ*). Absorption, specific to each excitation is used to quantify the analytes in a sample.

All UV-visible spectra of the samples in this thesis were recorded on the Agilent Cary 60 spectrophotometer model (shown in Figure 2.5) in the 200-700 nm wavelength range. Deuterium or hydrogen discharge tube and tungsten lamp are the two light sources in this spectrophotometer. For analysis, samples were appropriately diluted and taken in a quartz cuvette of 1 cm path length.

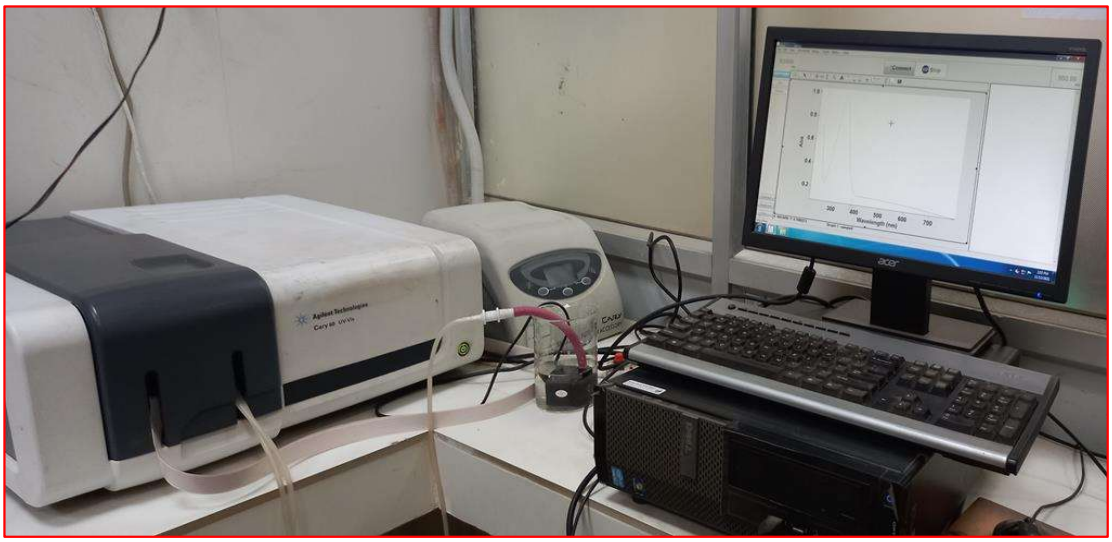

Figure 2.5 UV-Visible spectrophotometer (Model: Cary 60, Agilent).

2.2.1.6 UV-Vis diffuse reflectance spectroscopy (UV- DRS)

Solid-state UV–vis diffuse reflectance spectra were recorded in the 200-800 nm range on the Shimadzu company UV-2600 model displayed in Figure 2.6. The solid-state

absorbance data was used to find the optical bandgap of the prepared photocatalysts through the Tauc plot. The Tauc plots were constructed using the following relation.

$$(\alpha h\upsilon)^{1/n} = (h\upsilon - E_g) \quad (2.2)$$

The symbols α, υ, and E_g, in equation 2.2, denote the molar absorption coefficient, frequency of light, and material band gap, respectively. The intercept of the linear part of the Tauc plot of $(\alpha h\upsilon)^{1/n}$ versus hυ on the x-axis gives the photocatalyst's optical band gap (E_g) energy. The exponent n determines the nature of the optical transition. For indirect transition, the value of n is 2, whereas for a direct transition is 1/2.

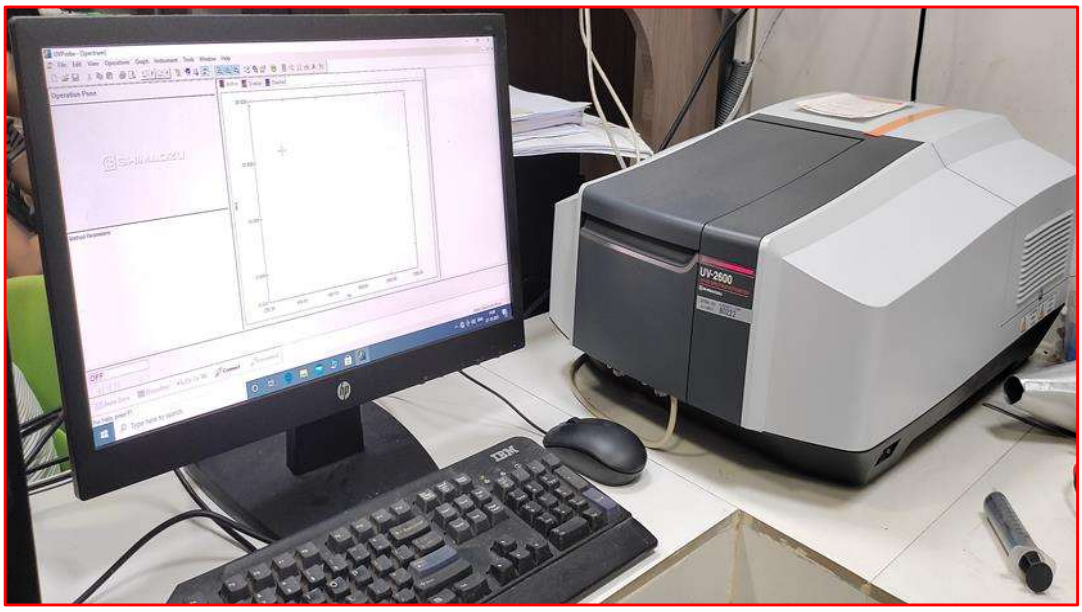

Figure 2.6 UV-Vis spectrophotometer with diffuse reflectance (Model: UV-2600, Shimadzu).

2.2.2 Procedures followed for Fenton and photo-Fenton catalytic activities

The Fenton and photo-Fenton catalytic activities of magnetite, starch functionalized magnetite, graphene oxide, and magnetite-graphene oxide composites were evaluated for the

degradation of two model pollutants (*p*-nitrophenol and orange-G). The detailed protocol used for catalytic Fenton and photo-Fenton degradation of model pollutants has been mentioned in Chapter 4, 5 and 6. The heterogeneously catalyzed Fenton reactions were carried out in the dark, while visible light irradiation was used for photo-Fenton reactions. The visible light source was a 14W(Philips) cool white LED bulb fixed in a homemade photocatalytic chamber. The TM-206 solar power meter (pyranometer) model was used to measure the cool white LED light's radiation flux density. The shape of a homemade photocatalytic chamber is a cubical box. The temperature inside the photocatalytic chamber was kept constant at 303 K during the reactions.

2.3 Computational part

2.3.1 Molecular Dynamics Simulations

The present section briefly introduces the key aspects of classical Molecular Dynamics (MD) simulations. Ab-initio molecular dynamics techniques have not been discussed because the thesis does not use them. The classical MD technique simulates the time evolution of position and velocity of a collection of interacting molecules by solving the Newton's laws of motion for each time instant. The first step in the MD simulation is to prepare the initial model system by stipulating the initial temperature, the number of molecules, density, and time step magnitude. Molecular mechanics, semi-empirical or ab-initio quantum mechanical techniques give the optimized molecular model. The investigator begins the simulation by specifying the initial position of molecules and the temperature. The criterion for selecting the initial system (the set of positions of molecules constituting the

system) configuration is that it should have a finite probability of occurrence under the given temperature and other ensemble conditions.

The key first step is the assignment of a force field to the planned MD simulation. Force fields are empirical potential energy expressions that enable the calculation of interactions between atoms in the system. At each step, the atoms' forces are calculated and combined with their current positions and velocities to create new positions and velocities. Verlet algorithm is a standard numerical integration algorithm for getting new positions and velocities[Allen & Tildesley (2017)]. Now, the atoms are moved to their new positions, the forces are updated, and a new cycle begins.

All simulations in this thesis invoke periodic boundary conditions with appropriate cut-offs. Periodic boundary condition requires that the central system (or simulation box) is surrounded by identical or replica simulation cells. Molecular movements in the central system are replicated in all surrounding mirror systems. Thus, if a molecule leaves the system from the right boundary of the central cell, then another molecule enters the system from its mirror system in the left. Sufficiently long-time simulations are carried out to generate valid ensemble averages. Hence, systems are first equilibrated for a sufficiently long run. The subsequent runtime is called the production run since the long time average over this data gives ensemble average properties of the system. The analysis of production run data can provide important information about the structural properties of the simulation system, such as radial distribution functions (RDF), adsorption properties (density profile, adsorption energies, hydrogen bonding), and dynamics properties (residence time) at the molecular level.

2.3.1.1 Ensemble

The MD calculations of the various adsorption properties studied in this thesis were performed in the NVT and NPT ensembles. In the NVT Ensemble (canonical ensemble), N is the number of particles, V is the volume, and the T temperature is kept constant. During the NVT simulations, the system is not thermally isolated, so that the total energy will fluctuate. However, this variation is proportional to $N^{1/2}$. The Nosé-Hoover thermostat implements this feature in simulations [Nosé, (1984), Hoover (1985)] done in this thesis. NPT ensemble requires that the system have a constant number of molecules, constant pressure and constant temperature [Andersen (1980)]. The unit cell vectors are allowed to change, and the pressure is adjusted by adjusting the volume. It is the ensemble of choice when the correct pressure, volume, and densities are critical in the simulation.

2.3.1.2 Force Field

The choice of the force field is an essential and primary step of MD simulations. The functional form of force field in terms of potential energy has two parts, i.e., bonded and non-bonded. The bonded energies consist of (a) stretching of atoms, (b) bond angle between atoms, (c) dihedral angle rotations. Non-bonded energies include van der Waals interactions (described by Lennard–Jones potential) and (e) electrostatic interactions (described by Coulomb's law). Dreiding [Mayo et al. (1990)] and the Universal (UFF) [Rappé et al. (1992)] are force fields that contain parameters for almost all classes of atoms in the periodic table. Another extensively used force field is the PCFF (polymer-consistent force field) [Sun et al. (1994)], parameterized against organic molecules containing heteroatoms, metal atoms, and zeolites. Thus, it is useful for organic and many inorganic materials. The condensed-phase

optimized molecular potentials for atomistic simulation studies (COMPASS) is another widely used computational force field model belonging to the same family of force fields as PCFF [Sun (1998)]. Note that the COMPASS force field is only available commercially and cannot be modified for a specific modeling requirement. This thesis uses SciPCFF (an extension of the PCFF force field) and Drieding to describe the interatomic interactions during MD simulations in different chapters.

2.3.1.3 Water Models

The present thesis applies molecular dynamics simulations to study the interfacial phenomena of adsorption of reactant molecules in the aqueous environment. Water plays a vital role in the simulation systems, so an accurate water model is necessary to obtain accurate MD simulation results. There are a large number of water models. Each water model fitted specifically a particular (condensed phase) structural feature or thermodynamic property of its physical counterpart. Three water models were used for simulations in this thesis work. The simulations in Chapter 3 used a (modified neglect of differential overlap) MNDO optimized three-point water model. MD simulations in chapters 4 and 6 used a modification of the (transferable intermolecular potential 4 point) TIP4P [Jorgensen et al. (1983)] water model. Note that MD simulations in these chapters used a three-body rigid water model with the (H-O-H) bond angle as per the TIP4P model. Then the charges on the atoms of this three-body model were replaced with the corresponding values in the TIP4P model. Chapter 5 used the simple point charge (SPC) [Berendsen et al. (1991)] water model.

The general scheme of steps generally followed in modeling a system for MD simulations is presented in Figure 2.7.

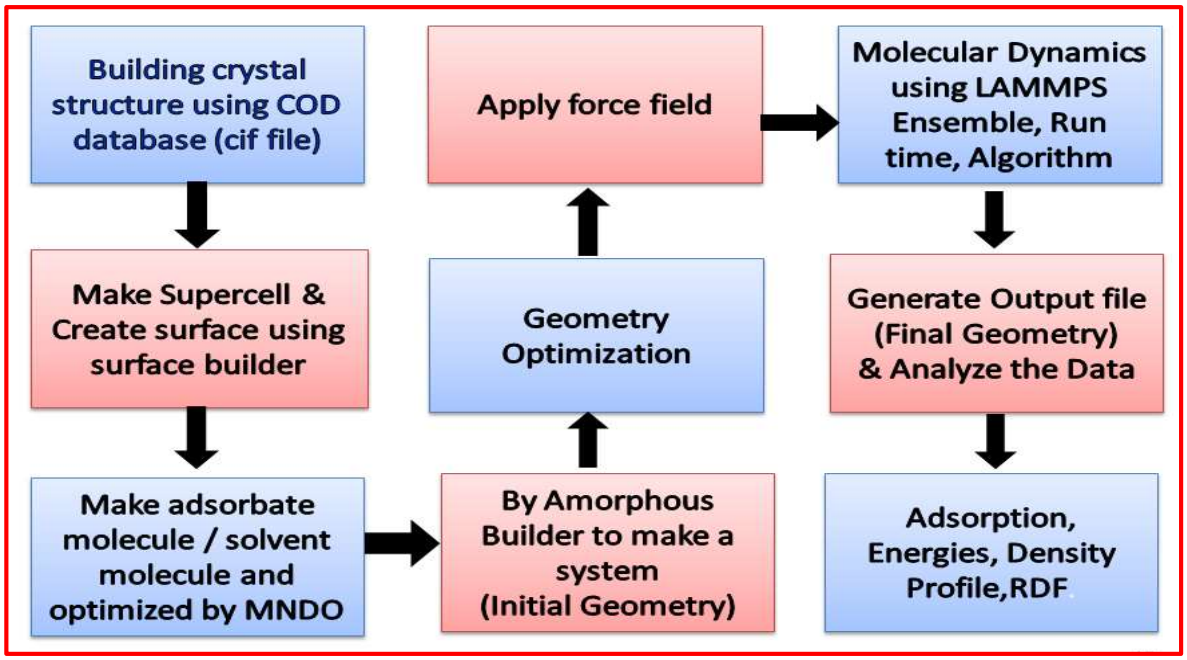

Figure 2.7 Basic methodology used in MD simulations.

2.3.1.4 Software used in Molecular Dynamics Simulations

In this thesis, LAMMPS (Large-scale Atomic/Molecular Massively Parallel System) software [Plimpton (1995)] is used to run MD calculations on the supercomputing system (PARAM SHIVAAY supercomputer) at IIT(BHU). For molecular modeling and analysis of results, MAPS (Materials and Process Simulation) software (released by SCIENOMICS) version 4.1.1 was used.

2.3.2 Quantum Mechanical calculations

The quantum mechanical calculations involve solving the Schrödinger's wave equation by either semi-empirical or ab-initio techniques or (density functional theory) DFT techniques.

$$H\Psi = E\Psi \qquad (2.3)$$

Equation 2.3, gives the Schrodinger wave equation. Here, H = Hamiltonian operator,

E = Energy eigenvalue, and Ψ = Wave function. The ab-initio techniques solve the Schrodinger wave function for a molecular system to obtain its energy and wave function. The latter can be utilized to determine all properties of a molecule. Semi-empirical approaches involve doing the same but requiring intermediate system-specific parameters/inputs for faster calculations. But these techniques suffer from inaccuracies for molecules that have not been parameterized for a particular method.

Density functional theory (DFT), a quantum mechanical method introduced by c, Kohn, and Sham (1960), determines the energy and molecular properties of the system from the electron density. The purpose of DFT is, therefore, to find the electron distribution of the simulated system directly [Hohenberg & Kohn (1964), Kohn & Sham (1965)]. DFT techniques are faster than ab-initio but slower than semi-empirical techniques. Like ab-initio approaches, it is not limited by parameterization requirements. Hence, the present thesis uses density functional theory (DFT) calculations and time-dependent density functional theory (TD-DFT) to calculate various electronic structure properties.

The TD-DFT calculations extend the basic ideas of the ground state DFT to the treatment of excited states based on the Runge–Gross theorem [Runge & Gross (1984), Casida (2009)]. The excitations energies were evaluated by the time-dependent self-consistent field (TD-SCF) method. The standard way to obtain such time-dependent density is through a modified version of the Kohn-Sham equation rewritten in terms of the time-dependent Schrödinger equation:

$$H(t)|\Psi(t)\rangle = i\frac{\partial}{\partial t}|\Psi(t)\rangle \qquad (2.4)$$

Here t denotes the time, $\Psi(t)\rangle$ the state vector of the quantum system, and H is the Hamiltonian operator.

In the present thesis work, TD-DFT has been used to calculate the excited states and modelled large molecules' UV/Vis absorption spectra [Jacquemin et al. (2011)]. The DFT and TD-DFT calculations enable us to obtain the locations of the frontier orbitals of molecules in the ground and excited states [Nakata et al. (2006)].

2.3.2.1 Basis set

Nobel laureate John Pople first developed the basis sets or mathematical functions to express wave functions and electron densities. A basis set determines calculation efficiency and accuracy[Hill (2013)]. This thesis used the 6-311++G (d,p) basis set for C, H and O atoms in magnetite and graphene oxide with LANL2DZ pseudopotentials on iron. The LANL2DZ, a double-zeta basis set, is frequently used in the study of transition metals. It is composed of the Los Alamos pseudopotential and double zeta valance basis set.

2.3.2.2 Functional

The popular hybrid functional B3LYP was used for all DFT calculations in this thesis. B3LYP is a combination of Becke's three-parameter (B3) [Becke (1998)] exchange functional. All geometry optimizations and excited-state calculations were performed using the functional B3LYP.

2.3.2.3 Software used in the Quantum Mechanical calculations

The calculations were carried out in the gas phase using the Gaussian 16 program installed on the computer server of the Centre for Computing and Information Services(CCIS), IIT BHU. Gaussview 6 software is used to draw and analyze the model. Lastly, obtained computational and experimental results were correlated.